

MODELING HEAT AND MOISTURE TRANSFER THROUGH BUILDING LOWER THERMAL BRIDGES

Gerson Henrique dos Santos, ghsantos@ufpr.br

Universidade Federal do Paraná - UFPR
Mechanical Engineering Graduate Program

Nathan Mendes, nathan.mendes@pucpr.br

Pontifícia Universidade Católica do Paraná - PUCPR
Mechanical Engineering Graduate Program

Abstract. *Multidimensional effects through porous building elements is normally disregarded by simulation tools due to many difficulties such as modeling complexity, computer run time, numerical convergence and highly moisture-dependent properties. Therefore, in order to analyze the effects of building lower thermal bridges, a multidimensional model has been developed to calculate the coupled heat, air and moisture transfer through building envelopes. The linearized set of discretized governing equations has been obtained by using the finite-volume method and was solved via the MultiTriDiagonal-Matrix Algorithm, improving substantially the numerical stability and reducing the computer run time. In the results section, the multidimensional effects in the lower thermal bridges formed by the soil, wall and floor are shown and analyzed in terms of temperature and relative humidity profiles.*

Keywords: *Thermal Bridges, Porous Media, Building Simulation*

1. INTRODUCTION

Residential, commercial and public buildings are greatly responsible for the total consumption of electricity, in a world-wide context. Only considering Brazil, they are responsible for at least 45%, which progressively motivates energy conservation studies for promoting building energy efficiency. In this context, to evaluate the building performance with thermal parameters, several codes have been developed. However, most of those codes do not take into account the moisture presence within building envelopes and the multidimensional effects. The moisture in building porous elements implies an additional mechanism of transport absorbing or releasing latent heat of vaporization, affecting the hygrothermal building performance, causing mold growth and structural damage.

Furthermore, when the multidimensional effect is considered, thermal bridges may play an important role. Thermal bridges appear in places where the envelope changes its geometry – such as corners and foundations - or material composition or both. Thermal bridge is used to define each part of the building envelope, where there is a local increase of heat flux density and a decrease or increase of internal surface temperatures. Beyond the thermal effect, the mass transport is also affected in the corner region and this fact is still barely explored in the literature due to as modeling complexity, computer run time, numerical convergence and highly moisture-dependent properties. However, around internal corners is where moisture can be easily accumulated and increase mold growth risks.

In a brief literature review, among the first works found in the literature, Brown and Wilson (1963) analyzed the insulation effect with some examples and illustrated factors that influence the thermal performance of the thermal bridges. Hassid (1990) proposed a correction to the one-directional heat transfer algorithms, to account for heat transfer across thermal bridges between parallel elements. In another work, Hassid (1991) implemented into the ESP building energy simulation program this model and showed to be able to predict the order of magnitude of changes due to corner effects and thermal bridges. These effects were not negligible to the prediction of internal surface temperature. In other important work, Deru (2003) cited that a well-built house is so energy efficient above ground that the ground-coupled heat losses can account for 30% to 50% of the total heat loss, showing the importance of a detailed analysis of ground coupled heat transfer.

In soil simulations, some parameters such as boundary conditions, initial conditions, simulation time period (including warm-up), simulation time step and grid refinement have to be carefully chosen and combined in order to reach accuracy without using excessive computational processing. Beyond this analysis, Santos and Mendes (2004) verified the importance of considering a three-dimensional approach for the soil domain for low-rise buildings, using a simply conductive model for ground heat transfer calculation.

Therefore, in order to analyze the heat and moisture transfer through building lower thermal bridges, a multidimensional model has been developed to calculate the coupled heat, air and moisture transfer through building envelopes. For ensuring numerical stability in the present model, the linearized set of equations has been obtained by using the finite-volume method and the MultiTriDiagonal-Matrix Algorithm (Mendes *et al.*, 2002) to solve a 2-D HAM model to describe the physical phenomena of heat, air and mass (HAM) transfer through porous building materials. In the results section, the multidimensional effects in the lower thermal bridges formed by the soil, wall and floor are shown and analyzed in terms of temperature and relative humidity profiles and vapor and heat flux for steady state condition through of the floor.

2. MATHEMATICAL MODEL

The model for the porous media domain has been elaborated considering the differential governing equations for moisture, air and energy balances. The transient terms of each governing equation have been written in terms of the driving potentials to take more advantage of the MTDMA (Mendes *et al.*, 2002) solution algorithm.

2.1 Moisture Transport

The moisture transport has been divided into liquid and vapor flows as shown in Eq. 1:

$$\mathbf{j} = \mathbf{j}_l + \mathbf{j}_v, \quad (1)$$

where \mathbf{j} is the density of moisture flow rate (kg/m²s), \mathbf{j}_l , the density of liquid flow rate (kg/m²s) and, \mathbf{j}_v , the density of vapor flow rate (kg/m²s).

The liquid transport calculation is based on the Darcy equation:

$$\mathbf{j}_l = K(\nabla P_{suc} - \rho_l \mathbf{g}), \quad (2)$$

where K is the liquid water permeability (s), P_{suc} , the suction pressure (Pa), ρ_l , the liquid water density (kg/m³) and \mathbf{g} the gravity (m/s²).

The capillary suction pressure can be written as a function of temperature and moisture content in the following form:

$$\nabla P_{suc} = \frac{\partial P_{suc}}{\partial T} \nabla T + \frac{\partial P_{suc}}{\partial P_v} \nabla P_v. \quad (3)$$

Similarly to the liquid flow, the vapor flow is calculated from the Fick's law based equation considering effects of both vapor pressure and air pressure driving potentials:

$$\mathbf{j}_v = -\underbrace{\delta_v \nabla P_v}_{\text{vapor diffusion}} - \rho_v \underbrace{\frac{kk_{rg}}{\mu_g} \nabla P_g}_{\text{convective vapor transport}}, \quad (4)$$

where δ_v is the vapor diffusivity (s), P_v , the partial water vapor pressure (Pa), ρ_v , the water vapor density (kg/m³), k , the absolute permeability (m²), k_{rg} , the gas relative permeability, μ_g , the dynamic viscosity (Pa.s) and, P_g , the gas pressure.

The water mass conservation equation can be described as:

$$\frac{\partial w}{\partial t} = -\nabla \cdot \mathbf{j}, \quad (5)$$

where w is the moisture content (kg/m³).

This moisture content conservation equation – Eq. 5 – can be written in terms of the three driving potentials as:

$$\frac{\partial w}{\partial \phi} \frac{\partial \phi}{\partial P_v} \frac{\partial P_v}{\partial t} + \frac{\partial w}{\partial \phi} \frac{\partial \phi}{\partial T} \frac{\partial T}{\partial t} = \nabla \cdot \left[-K \frac{\partial P_{suc}}{\partial T} \nabla T - \left(K \frac{\partial P_{suc}}{\partial P_v} - \delta_v \right) \nabla P_v + \rho_v \frac{kk_{rg}}{\mu_g} \nabla P_g + K \rho_l \mathbf{g} \right]. \quad (6)$$

2.2 Air Transport

In the proposal model, the air transport is individually considered through the dry-air mass balance. In this way, the dry-air conservation equation can be expressed as:

$$\frac{\partial \rho_a}{\partial t} = -\nabla \cdot \mathbf{j}_a, \quad (7)$$

with the air flow calculated by the following expression:

$$\mathbf{j}_a = \underbrace{\delta_v \nabla P_v}_{\text{air diffusion}} - \rho_a \underbrace{\frac{kk_{rg}}{\mu_g} \nabla P_g}_{\text{air convection}}, \quad (8)$$

where ρ_a is the density of dry air (kg/m^3), \mathbf{j}_a , the density of dry air flow rate ($\text{kg/m}^2\text{s}$) and, P_g , the gas pressure (dry air pressure plus vapor pressure) in Pa.

Therefore, the dry air transport can be described as a function of the partial gas and vapor pressure driving potentials so that the air balance can be written as:

$$\frac{\partial \rho_a}{\partial P_g} \frac{\partial P_g}{\partial t} + \frac{\partial \rho_a}{\partial P_v} \frac{\partial P_v}{\partial t} + \frac{\partial \rho_a}{\partial T} \frac{\partial T}{\partial t} = \nabla \cdot \left(-\delta_v \nabla P_v + \rho_a \frac{kk_{rg}}{\mu_g} \nabla P_g \right). \quad (9)$$

2.3 Heat Transport

The heat transfer can be attributed to both conductive and convective effects. The conductive transport is calculated by the Fourier's law:

$$\mathbf{q}_{\text{cond}} = -\lambda \nabla T, \quad (10)$$

while the convective transport can be written as:

$$\mathbf{q}_{\text{conv}} = \underbrace{\mathbf{j}_l c_{pl} T}_{\text{liquid flow}} + \underbrace{\mathbf{j}_a c_{pa} T}_{\text{dry air flow}} + \underbrace{\mathbf{j}_v L}_{\text{phase change}} + \underbrace{\mathbf{j}_v c_{pv} T}_{\text{vapor flow}}, \quad (11)$$

where λ is the thermal conductivity (W/mK), c_{pa} , the specific heat capacity at constant pressure of the dry air (J/kgK), c_{pl} , the specific heat capacity of the water liquid (J/kgK), c_{pv} , the specific heat capacity at constant pressure of the vapor (J/kgK) and, L , the vaporization latent heat (J/kg).

The energy balance equation can be described as:

$$c_m \rho_0 \frac{\partial T}{\partial t} = -\nabla \cdot \mathbf{q}, \quad (12)$$

where c_m is the specific heat capacity of the structure (J/kgK) and ρ_0 , the density of the dry material (kg/m^3).

In this way, assuming 0°C as the reference temperature, the energy conservation equation can be written in terms of the three driving potentials as:

$$c_m \rho_0 \frac{\partial T}{\partial t} = \nabla \cdot \left(\left(\left(\lambda - K \frac{\partial P_{suc}}{\partial T} c_{pl} T \right) \nabla T - \left(K \frac{\partial P_{suc}}{\partial P_v} c_{pl} T + \delta_v c_{pa} T - \delta_v (L + c_{pv} T) \right) \nabla P_v + \left(\rho_a \frac{kk_{rg}}{\mu_g} c_{pa} T + \rho_v \frac{kk_{rg}}{\mu_g} (L + c_{pv} T) \right) \nabla P_g + K \rho_l c_{pl} T \mathbf{g} \right) \right). \quad (13)$$

2.4 Boundary Conditions

In the dry-air conservation equation of the present model, gas pressure has been considered as a prescribed value – Dirichlet condition - at the envelope surface:

$$P_{g,\infty} = P_{g,\text{sup}}. \quad (14)$$

For the moisture flow, vapor transport is considered due to the difference between the partial vapor pressure in air and at the external and internal surfaces:

$$j = \beta_v(p_{v,\infty} - p_{v,\text{sup}}), \quad (15)$$

where j is the density of moisture flow rate (kg/m²s) and β_v the surface coefficient of water vapor transfer (s/m), calculated from the Lewis' relation.

For the heat transport convection heat transfer and phase change were considered:

$$q = h(T_\infty - T_{\text{sup}}) + \beta_v(p_{v,\infty} - p_{v,\text{sup}})L(T), \quad (16)$$

where q is the heat flowing into the structure (W/m²) and h the convective heat transfer coefficient (W/m²K).

3. SOLUTION OF THE BALANCE EQUATIONS

A fully-implicit central-difference scheme has been considered for the discretization using the finite-volume method (Patankar, 1980) for the governing equations and the MTDMA to simultaneously solve the three set of equations as previously described in the porous element domain section.

3.1 Discretized Conservation Equations Solution of the Porous Element Domain

Implicit schemes demand the use of an algorithm to solve tridiagonal systems of linear equations. One of the most used is the well-known Thomas Algorithm or TDMA (TriDiagonal-Matrix Algorithm). However, for strongly-coupled equations of heat and mass transfer problems, a more robust algorithm may be necessary in order to achieve numerical stability (Mendes and Philippi, 2004).

For a physical problem represented by M dependent variables, the discretization of $M \times N$ differential equations, leads to the following system of algebraic equations,

$$\mathbf{A}_i \cdot \mathbf{x}_i = \mathbf{B}_i \cdot \mathbf{x}_{i+1} + \mathbf{C}_i \cdot \mathbf{x}_{i-1} + \mathbf{E}_i \quad (17)$$

where \mathbf{x} is a vector containing the M dependent variables T , P_v and P_g

$$\mathbf{x}_i = \begin{bmatrix} T \\ P_v \\ P_g \end{bmatrix}. \quad (18)$$

Differently from the traditional TDMA, coefficients \mathbf{A} , \mathbf{B} and \mathbf{C} are $M \times M$ matrices, in which each line corresponds to one dependent variable. The elements that do not belong to the main diagonal are the coupled terms for each conservation equation. \mathbf{E} is an M -element vector.

As MTDMA has the same essence as TDMA, it is necessary to replace Eq. (17) by relationships of the form

$$\mathbf{x}_i = \mathbf{P}_i \cdot \mathbf{x}_{i+1} + \mathbf{q}_i, \quad (19)$$

where \mathbf{P}_i is now a $M \times M$ matrix.

The use of this algorithm makes the systems of equations to be more diagonally dominant and the diagonal dominance is improved by the fact that the \mathbf{A}_i coefficients are increased at the same time the \mathbf{E}_i source terms are decreased. Therefore, the transient terms of the Eqs. 6 and 9 also were written thus to increase the diagonal dominance.

4. SIMULATION PROCEDURE

In order to focus on the lower thermal bridge, the domain (Fig. 1) - divided into square cells of a regular Cartesian mesh - has been considered for all simulations. A 0.1-m thickness brick wall and floor has been used. The hygrothermal properties have been obtained from the benchmark of the European project HAMSTAD (Hagentoft, 2002), for brick (wall and floor), and from Oliveira *et al.* (1993), for a sandy silt soil.

In the winter condition, at the upper surface of the soil and left surface of the wall, constant uniform values of 10 W/m²K, 288 K and 80% have been considered for the convective heat transfer coefficient, external temperature and relative humidity, respectively. On the other hand, in the summer condition, 303 K was adopted for the temperature. The other properties have been kept constant.

Internally, at the upper surface of the floor and right surface of the wall, constant uniform values of 3 W/m²K, 297 K and 50% have been considered for the convective heat transfer coefficient, external temperature and relative humidity, respectively, for an air conditioned environment. The other surfaces have been considered adiabatic and impermeable. As initial conditions for the whole domain, temperature, relative humidity and gas pressure of 293 K, 50% and 100 kPa have been assumed in order to represent the winter conditions. For summer condition, only the initial temperature was changed to 298 K.

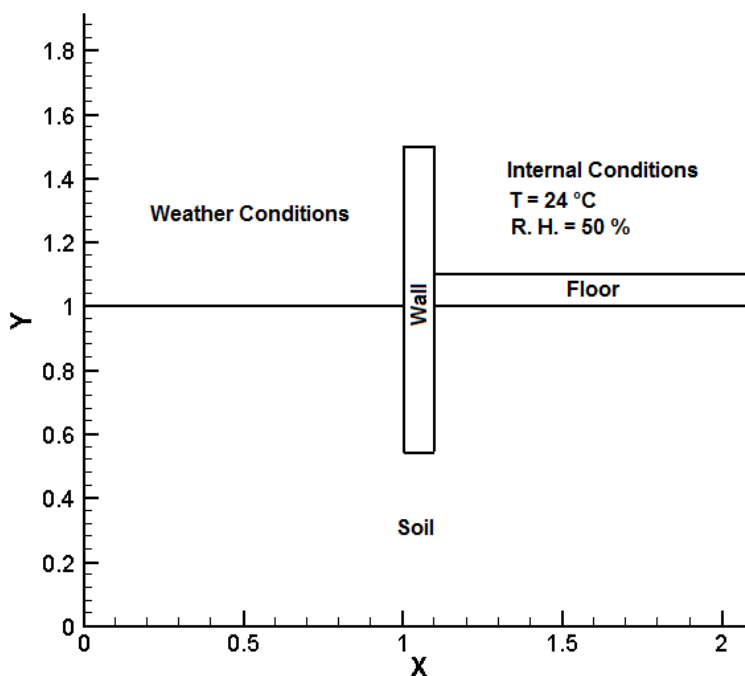


Figure 1. Physical domain of the lower corner (dimensions in meter).

5. RESULTS

In Figs. 2 and 3, temperature and relative humidity profiles are presented, after 1 year of simulation. The multidimensional effects in the profiles are verified due to thermal bridges caused by geometry and different structure compositions. At the interface between the wall and the floor, a local increase on heat flux density and a decrease on internal surface temperatures have been observed (winter condition). An increase on the relative humidity in this region has also been noticed, which may cause structural damage due to moisture infiltration when the foundation is not properly sealed.

In Fig. 3, lower values of relative humidity are observed at the internal surfaces when compared to the results presented in Fig. 2. This reduction is attributed to an increase on the internal surface temperature.

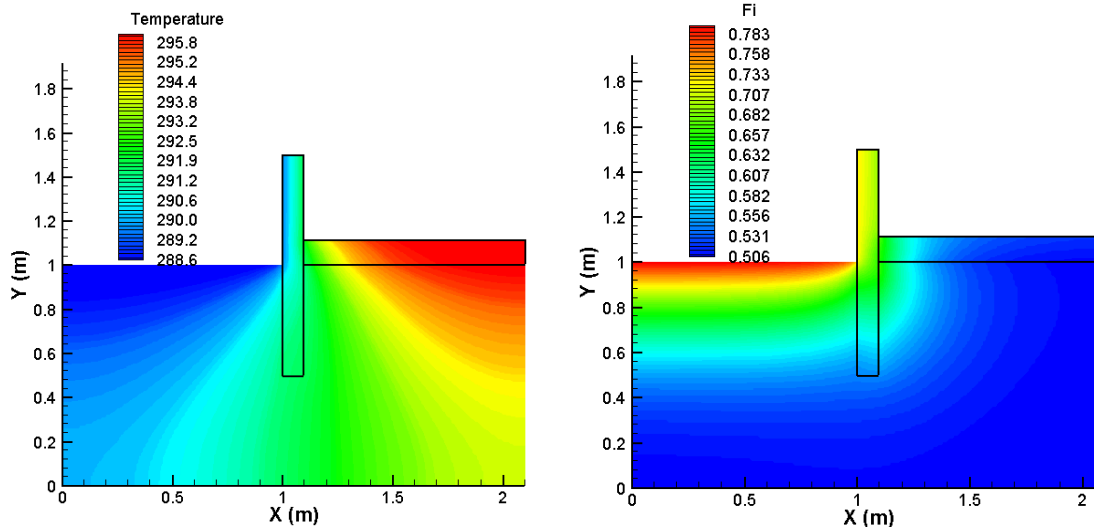


Figure 2. Temperature (K) and relative humidity profiles within the domain (winter condition).

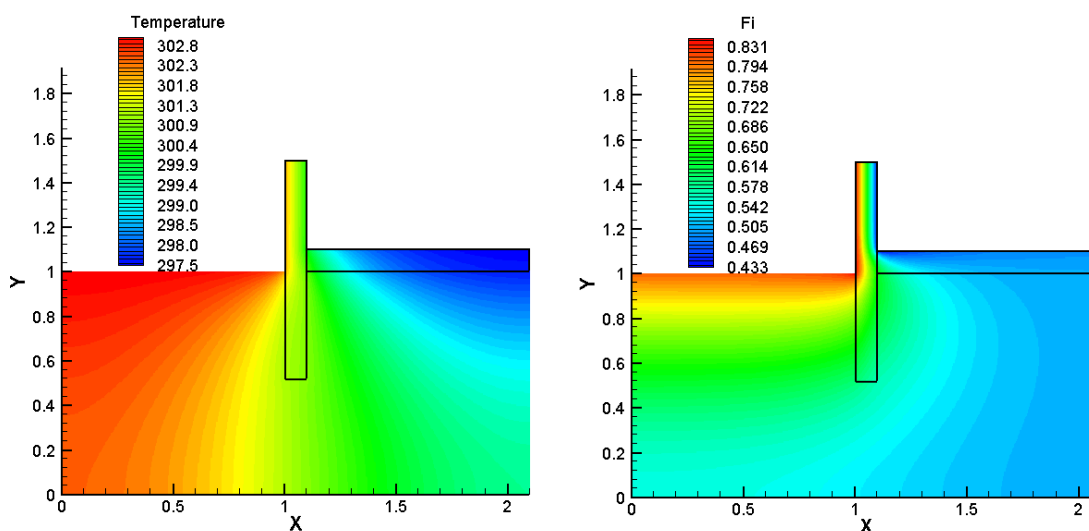


Figure 3. Temperature (K) and relative humidity profiles within the domain (summer condition).

Table 1 presents the vapor and heat flux values for steady state condition through the floor internal surface. The minus sign indicates that the flux is in the porous media direction. The multidimensional effect is compared to the one-dimensional case. For both conditions (winter and summer), a significant variation on the total heat flux values have been verified. A higher difference on the vapor flux has been observed for the summer condition due to vapor pressure increase at the upper floor surface. Results have also shown that the building perimeter may cause great influence on the thermal load from the floor, which can be reduced by increasing insulation thermal resistance in the foundation, as widely used in Europe (Krarti, 1994).

Table 1. Vapor and heat flux values for steady state conditions through the floor.

Condition	Vapor Flux (kg/m ² s)	Sensible Heat Flux (W/m ²)	Latent Heat Flux (W/m ²)	Total Heat Flux (W/m ²)
2-D Lower Corner (Winter)	-2.739E-08	-3.92	-0.068	-3.99
1-D (Winter)	-2.872E-08	-1.68	-0.071	-1.75
2-D Lower Corner (Summer)	1.263E-07	2.72	0.320	3.04
1-D (Summer)	2.837E-08	1.26	0.070	1.33

6. CONCLUSIONS

In order to analyze the effects of building lower thermal bridges, a multidimensional model has been developed to calculate the coupled heat, air and moisture transfer through building envelopes. In the results section, the multidimensional effects in the lower thermal bridges formed by the soil, wall and floor has been presented. In the winter condition, a local increase on the heat flux density and a decrease on the internal surface temperatures have been observed at the interface between the wall and the floor. An increase on the relative humidity in this region has also been noticed. For the summer condition, a higher difference on the vapor flux has been observed due to the vapor pressure increase at the upper floor surface.

Due to the high computer run time, other boundary conditions, simulation time period (including warm-up), simulation time step and grid refinement effects will be presented in a next article.

7. ACKNOWLEDGEMENTS

The authors thank CNPq – Conselho Nacional de Desenvolvimento Científico e Tecnológico – of the Secretary for Science and Technology of Brazil and Centrais Elétricas do Brasil - Eletrobras.

8. REFERENCES

- Brown, W. P., Wilson, A. G., 1963. CBD-44. Thermal Bridges in Buildings. http://irc.nrc-cnrc.gc.ca/pubs/cbd/cbd044_e.html
- Deru, M., 2003. A Model for Ground-Coupled Heat and Moisture Transfer from Buildings. Technical Report. National Renewable Energy Laboratory.
- Hagentoft, C. E., 2002. HAMSTAD – WP2 Modeling, Report R-02:9. Gothenburg, Department of Building Physics, Chalmers University of Technology.
- Hassid, S., 1990. Thermal Bridges Across Multilayer Walls: An Integral Approach. *Building and Environment*, Vol. 25, pp. 143-150.
- Hassid, S., 1991. Algorithms for Multi-Dimensional Heat Transfer in Buildings. International IBPSA Conference, pp. 9-13.
- Krarti, M., 1994. Heat Loss and Moisture Condensation for Wall Corners. *Energy Conversion and Management*, Vol. 35, N. 8, pp. 651-659.
- Mendes, N., Philippi, P. C., Lamberts, R. A., 2002. New Mathematical Method to Solve Highly Coupled Equations of Heat and Mass Transfer in Porous Media. *Int. Journal of Heat and Mass Transfer*, Vol. 45, pp. 509-518.
- Mendes, N., Philippi, P. C., 2004. MultiTriDiagonal-Matrix Algorithm for Coupled Heat Transfer in Porous Media: Stability Analysis and Computational Performance. *Journal of Porous Media*, Vol. 7, N. 3, pp. 193-211.
- Oliveira Jr, A. A. M., Freitas, D. S., Prata, A. T., 1993. Influência das Propriedades do Meio nas Difusividades do Modelo de Phillip e de Vries em Solos Insaturados. Relatório de Pesquisa. UFSC.
- Patankar S.V., 1980. *Numerical Heat Transfer and Fluid Flow*, Hemisphere Publishing Corporation, 1980.
- Santos, G. H., Mendes, N., 2003. Multidimensional Effects of Ground Heat Transfer on the Dynamics of Building Thermal Performance. *ASHRAE Transactions*. Vol. 110, pp.345-354.

9. RESPONSIBILITY NOTICE

The authors are the only responsible for the printed material included in this paper.